


Prevalent Introgression Underlies Convergent Evolution in the Diversification of *Pungitius* Sticklebacks

Yu Wang,^{1,2} Yingnan Wang,¹ Xiaoqi Cheng,^{1,2} Yongli Ding,^{1,2} Chongnv Wang,¹ Juha Merilä,^{3,4} and Baocheng Guo ^{1,2,5,6,*}

¹Key Laboratory of Zoological Systematics and Evolution, Institute of Zoology, Chinese Academy of Sciences, Beijing, China

²University of Chinese Academy of Sciences, Beijing, China

³Ecological Genetics Research Unit, Research Programme in Organismal and Evolutionary Biology, Faculty of Biological and Environmental Sciences, University of Helsinki, Helsinki, Finland

⁴Area of Ecology and Biodiversity, School of Biological Sciences, The University of Hong Kong, Hong Kong SAR, China

⁵Center for Excellence in Animal Evolution and Genetics, Chinese Academy of Sciences, Kunming, China

⁶Academy of Plateau Science and Sustainability, Qinghai Normal University, Xining, China

*Corresponding author: E-mail: guobaocheng@ioz.ac.cn.

Associate editor: Sophie von der Heyden

Abstract

New mutations and standing genetic variations contribute significantly to repeated phenotypic evolution in sticklebacks. However, less is known about the role of introgression in this process. We analyzed taxonomically and geographically comprehensive genomic data from *Pungitius* sticklebacks to decipher the extent of introgression and its consequences for the diversification of this genus. Our results demonstrate that introgression is more prevalent than suggested by earlier studies. Although gene flow was generally bidirectional, it was often asymmetric and left unequal genomic signatures in hybridizing species, which might, at least partly, be due to biased hybridization and/or population size differences. In several cases, introgression of variants from one species to another was accompanied by transitions of pelvic and/or lateral plate structures—important diagnostic traits in *Pungitius* systematics—and frequently left signatures of adaptation in the core gene regulatory networks of armor trait development. This finding suggests that introgression has been an important source of genetic variation and enabled phenotypic convergence among *Pungitius* sticklebacks. The results highlight the importance of introgression of genetic variation as a source of adaptive variation underlying key ecological and taxonomic traits. Taken together, our study indicates that introgression-driven convergence likely explains the long-standing challenges in resolving the taxonomy and systematics of this small but phenotypically highly diverse group of fish.

Key words: phylogenomics, convergence, parallelism, adaptive introgression, SNPs.

Introduction

Understanding the extent to which evolution is repeatable and predictable is a central goal in evolutionary biology (Darwin 1859). Convergence—the independent evolution of similar phenotypes at intraspecific and/or interspecific levels—provides opportunities to investigate evolutionary repeatability and predictability at different hierarchical levels (Stern 2013; Rosenblum et al. 2014). For example, the three-spined stickleback (*Gasterosteus aculeatus*) is a supermodel for the study of repeated evolution in the wild (Gibson 2005; Hendry et al. 2013), since this species has repeatedly colonized freshwater habitats from the sea throughout the northern hemisphere, and evolved similar changes in morphological, physiological, life history, and behavioral traits (Bell and Foster 1994). The repeated adaptation to freshwater in three-spined sticklebacks is often underlain by genetic parallelism—parallel phenotypes resulting from similar molecular mechanisms (Peichel and Marques 2017; but see Fang et al. 2020).

However, the sources of parallel genetic changes underlying different parallel phenotypes in freshwater three-spined sticklebacks are not necessarily identical: they can be underlined by repeated selection on either new mutations that have occurred in freshwater populations, or by standing genetic variation existing in ancestral marine populations. For example, the reduction of the pelvic apparatus in freshwater three-spined sticklebacks, a hallmark repeated phenotypic change associated with freshwater colonization, results from the recurrent deletion of the same *Pitx1* enhancer of *Pel* (Chan et al. 2010). Unlike *Pel* deletions, which occur at elevated rates due to its DNA fragility and sweep rapidly to fixation, most new mutations (e.g., single-nucleotide mutations) usually occur at low rates with neutral or small effects, and are either lost or rise to fixation slowly (Xie et al. 2019). Therefore, repeated selection on new mutations alone is unlikely to explain the prevalence of genetic parallelism leading to the large set of genome-wide loci consistently associated with repeated

© The Author(s) 2023. Published by Oxford University Press on behalf of Society for Molecular Biology and Evolution.

This is an Open Access article distributed under the terms of the Creative Commons Attribution-NonCommercial License (<https://creativecommons.org/licenses/by-nc/4.0/>), which permits non-commercial re-use, distribution, and reproduction in any medium, provided the original work is properly cited. For commercial re-use, please contact journals.permissions@oup.com

Open Access

marine-freshwater divergence in three-spined sticklebacks (Hohenlohe et al. 2010; Jones et al. 2012).

On the contrary, repeated selection on standing genetic variation in marine three-spined sticklebacks increases the probability of genetic parallelism in adaptation to freshwater environments (Barrett and Schluter 2008). Lateral plate reduction in freshwater three-spined sticklebacks, another hallmark of repeated phenotypic change in response to freshwater colonization, is a result of repeated selection on pre-existing genetic variation in the *Eda* gene—the major locus underlying lateral plate reduction in marine three-spined sticklebacks (Colosimo et al. 2004, 2005; Cresko et al. 2004). Marine populations contain a low frequency of the same freshwater *Eda*-alleles, which repeatedly increase in frequency in freshwater populations (Colosimo et al. 2005). Selection on pre-existing genetic variation in marine sticklebacks has also been demonstrated in the repeated evolution of other traits in freshwater populations (e.g., pigmentation; Miller et al. 2007). Furthermore, parallel adaptation in geographically isolated freshwater populations has consistently involved fixation of identical-by-descent ancient haplotypes spread broadly across the three-spined stickleback genome (Nelson and Cresko 2018). Schluter and Conte (2009) proposed the “transporter hypothesis” to explain the prevalence and rapid evolution of genetic parallelism in the repeated adaptation to freshwater in this species. This hypothesis postulates that selection in freshwater environments repeatedly acts on standing genetic variation that is maintained in marine populations by recurrent export of freshwater-adapted alleles from previously colonized freshwater populations. The transporter hypothesis highlights the importance of gene flow in genetic parallelism when three-spined sticklebacks colonize freshwater environments.

The genetic parallelism underlying similar phenotypic shifts in sticklebacks is not limited to three-spined sticklebacks at the intraspecific level, but is also found among sticklebacks at the interspecific level. As in three-spined sticklebacks, the *Pitx1* gene is also responsible for the repeated pelvic reduction in some nine-spined stickleback (*Pungitius pungitius*) populations (Shapiro et al. 2006; Shikano et al. 2013), although alternative candidate genes exist in other populations (Shapiro et al. 2009; Kemppainen et al. 2021). In fact, repeated reduction of body armor traits (e.g., pelvic apparatus and lateral plates) is frequently observed in *Pungitius* sticklebacks, whereas there is no correspondence between the mitochondrial sequence-based phylogeny and the occurrence of distinct armor phenotypes within this genus (Keivany and Nelson 2000, 2004; Wang et al. 2015; Denys et al. 2018; Guo et al. 2019). Therefore, body armor traits as taxonomically diagnostic traits are subject to extensive homoplasy and likely result in the long-standing taxonomic conundrum in *Pungitius* sticklebacks (Guo et al. 2019). Due to the existence of a partially plated morph—a typical character in *P. pungitius*—*Pungitius sinensis* in Hokkaido and Honshu, Japan, was incorrectly recognized as a freshwater type of

P. pungitius until recently (Takahashi and Goto 2001; Takahashi et al. 2001, 2016; Ishikawa et al. 2013; Guo et al. 2019; Natri et al. 2019). Such taxonomically erroneous assignment also exists in the *P. pungitius*–*Pungitius kaibarae* stickleback complex in Japan (Tsuruta and Goto 2006; Takahashi et al. 2016; Guo et al. 2019; Natri et al. 2019) and in the *P. pungitius*–*Pungitius laevis* stickleback complex in France (Keivany and Nelson 2000; Wang et al. 2015, 2017). Remarkably, historical gene flow has been found between *Pungitius* sticklebacks involved in the abovementioned taxonomic conundrums (Takahashi et al. 2016; Wang et al. 2017; Guo et al. 2019; Yamasaki et al. 2020). Therefore, gene flow might contribute to genetic parallelism underlying convergence in *Pungitius* sticklebacks at the interspecific level. This seems plausible, given that introgression has been increasingly recognized as a critically important source of genetic variation in adaptation and diversification (Hedrick 2013; Arnold and Kunte 2017; Suarez-Gonzalez et al. 2018; Burgarella et al. 2019; Taylor and Larson 2019; Edelman and Mallet 2021). However, little is known about the genomic footprints of historical gene flow and its impact on the diversification of *Pungitius* sticklebacks (Yamasaki et al. 2020; Feng et al. 2022).

To investigate the role of hybridization and introgression in the diversification of *Pungitius* sticklebacks, we conducted taxonomically and geographically diverse sampling on a global scale and reconstructed their phylogeny with comprehensive genomic data. We then identified introgression scenarios in the diversification of *Pungitius* sticklebacks and characterized genomic footprints of introgression in current *Pungitius* stickleback genomes. We further deciphered the impact of introgression in genetic variation in core gene regulatory networks underlying two phenotypic traits of adaptive significance—pelvic girdle and lateral plate reduction. Our findings indicate that introgression has likely been an important source of genetic variation facilitating genetic parallelism and phenotypic convergence in *Pungitius* sticklebacks, and also explains some of the difficulties faced by *Pungitius* taxonomy, which has relied heavily on traits impacted by introgression.

Materials and Methods

Sample Collection

Genomic data were used from 169 *Pungitius* individuals representing 10 of the 12 currently recognized *Pungitius* species, collected from 68 global sampling sites (fig. 1A; supplementary table S1, Supplementary Material online). Genomic data from six other sticklebacks were also included to provide outgroup material (supplementary table S1, Supplementary Material online). The fish were captured with hand seines and/or minnow traps and preserved in ethanol after over-anesthetizing with tricaine methane sulfonate. The fish were sampled in accordance with the national legislation of the countries concerned, under ethical licenses granted to collectors listed in

Acknowledgments. Detailed information on the individuals sampled in this study are given in [supplementary table S1, Supplementary Material](#) online.

Sequencing and Genotype Calling

Whole-genome sequencing (WGS) and restriction site-associated DNA sequencing (RAD-seq) were performed for 19 and 41 *Pungitius* individuals sampled in this study, respectively. DNA extraction, library construction, and sequencing strategy for WGS and RAD-seq are given in detail in [Wang et al. \(2022\)](#) and [Guo et al. \(2019\)](#). Published WGS and RAD-seq data for an additional 109 *Pungitius* individuals and six individuals of three outgroup species from earlier studies ([Guo et al. 2019](#); [Yamasaki et al. 2020](#); [Feng et al. 2022](#); [Wang et al. 2022](#)) were retrieved from GenBank ([supplementary table S1, Supplementary Material](#) online). Raw sequencing read quality assessment and filtering for each sample was done using FastQC and FastX toolkits, respectively. Qualified sequencing reads were aligned to the *P. pungitius* reference genome ([Varadharajan et al. 2019](#)) using the MEM algorithm of Burrows–Wheeler Aligner (BWA; [Li and Durbin 2010](#)). BAM format alignment files were sorted and indexed using SAMtools ([Li 2011](#)). The number of aligned read pairs ranged from 1.1 to 15.5 million per individual, with a mapping ratio between 50.9% and 98.9% ([supplementary table S1, Supplementary Material](#) online). After read sorting and duplicate removal, single-nucleotide polymorphisms (SNPs) were called using BCFtools ([Li 2011](#)) and SAMtools. Finally, the following filtering criteria were applied to the raw variants using the VCFtools ([Danecek et al. 2011](#)). After filtering SNPs with (1) genotype and/or mapping quality below 20, (2) located ≤ 10 bp from any indels, or (3) in linkage group (LG) 12 (sex chromosome in *P. pungitius*; [Shikano et al. 2011](#)), 1,073,966 biallelic SNPs existing in at least 90% of individuals with minor allele frequency > 0.05 were used in the subsequent phylogenetic and introgression inferences.

Phylogenetic Inference and Divergence Time Estimation

A maximum likelihood phylogenetic tree for 10 *Pungitius* species was inferred using IQ-TREE ([Nguyen et al. 2015](#)) with 1,073,966 SNPs from 126 *Pungitius* individuals from 66 worldwide sampling sites and six individuals of three outgroup species. The generalized time-reversible model with gamma-distributed rate variation with invariable sites (GTR + Gamma + I) was used as the best-fitting nucleotide substitution model according to ModelFinder ([Kalyanamoorthy et al. 2017](#)), and node support was obtained by performing 100 ultrafast bootstrap replicates. A Bayesian molecular clock approach was used for species divergence time estimation with SNAPP package ([Bryant et al. 2012](#)) in BEAST2 ([Bouckaert et al. 2014](#)). Two calibration points were used in divergence time estimation: divergence time of 26 Ma between *P. pungitius* and *G. aculeatus* ([Varadharajan et al. 2019](#)), and the earliest *Pungitius* spp.

fossil record of 7 Ma ([Rawlinson and Bell 1982](#); [Bae and Suk 2015](#)) as the minimum time to the most recent common ancestor for *Pungitius* taxa. Associations between phylogenies (both mitochondrial and nuclear data based) and armor traits (presence or absence of lateral plates, pelvic apparatus, and keel) were tested using phylo.d ([Fritz and Purvis 2010](#)) in the R package caper (<https://cran.r-project.org/web/packages/caper/index.html>) by following the strategy outlined in [Wang et al. \(2015\)](#).

Detecting Admixture

To disentangle whether cytonuclear discordance in *Pungitius* sticklebacks resulted from introgression and/or incomplete lineage sorting (ILS), the “InferNetwork_ML” function ([Yu et al. 2014](#)) in PhyloNet ([Than et al. 2008](#)) was used to compare the likelihoods of gene trees under ILS alone and species trees with migration event by adding a single introgression edge. In each tested scenario, gene trees were obtained with 10-kb genomic regions with no < 50 SNPs on the 20 autosomal LGs in the *P. pungitius* reference genome using IQ-TREE. Species in the gene tree were reduced to a single representative population in all PhyloNet analyses. To exclude topologically uncertain nodes in the gene tree, ultrafast bootstrap node support ≥ 0.9 was required with the option “-b.” Ten replicates in each test scenario were performed for all gene trees with the option “-x.” Branch length and inheritance probability of introgression edge were optimized to compute likelihoods for each proposed network with the option “-o.” Networks were visualized with *IcyTree* (<https://icytree.org>). Patterson’s *D*, also known as the ABBA-BABA statistic ([Durand et al. 2011](#)), was then used to detect possible historical gene flow between *Pungitius* species and quantify genome-wide admixture proportion in the nuclear genome using Dsuite ([Malinsky et al. 2021](#)). Patterson’s *D* statistic applies to a four-taxon asymmetric phylogeny with three ingroup taxa and an outgroup, denoted as (((P1, P2), P3), O), in which the frequencies of sharing a derived allele “B” relative to the outgroup between P3 and P2 (ABBA) and between P3 and P1 (BABA) should be equal if there is no gene flow between P2 and P3. To polarize the direction of gene flow, D_{FOIL} tests of an integrated framework were adopted to infer both the taxa involved and the direction of introgression with a symmetric five-taxon phylogeny ([Pease and Hahn 2015](#)). By accounting for introgression events detected by Patterson’s *D* statistic, a symmetric phylogeny of five *Pungitius* species/population as (((P1, P2), (P3, P4)), O) with two subpairs of ingroup taxa (P1/P2 and P3/P4) and an outgroup taxon was determined to infer the direction of introgression between each pair of the ingroup taxa, between P3 and ancestor of P1 and P2, and between P4 and ancestor of P1 and P2 in each introgression event between *Pungitius* sticklebacks.

Deciphering Genome-wide Footprint of Introgression

To characterize genome-wide footprint of introgression in each introgression event between *Pungitius* sticklebacks,

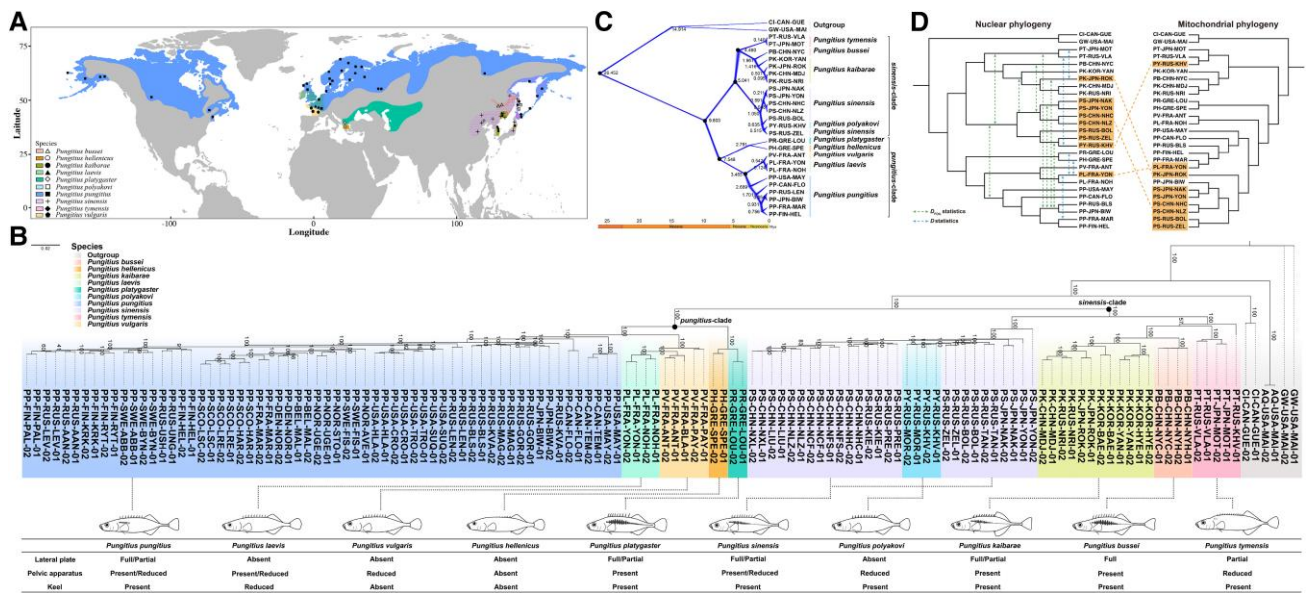


FIG. 1. The global diversification of *Pungtius* sticklebacks. (A) The worldwide distribution of *Pungtius* sticklebacks and sampling localities of this study. (B) Maximum likelihood phylogeny of *Pungtius* sticklebacks based on genome-wide SNPs. Numbers at nodes are bootstrap values. Armor traits are retrieved from earlier studies (Wang et al. 2015; Takahashi et al. 2016; Guo et al. 2019). (C) The time-calibrated phylogeny of major *Pungtius* stickleback lineages obtained with SNAPP. (D) Admixture scenarios based on Patterson’s *D* and *D*_{FOIL} statistics and cytonuclear discordances in *Pungtius* sticklebacks.

*D*_{FOIL} tests were first performed across the 20 autosomal LGs in the reference genome with a 100-kb nonoverlapping window, excluding the top 5% 100-kb nonoverlapping windows with low or high number of SNPs. To trace the ancestry of discrete genomic segments (ancestry tracts) in recipient population back to the ancestral populations from which they are derived, a local ancestry inference method based on coalescent theory was additionally adopted using Ancestry_HMM (Medina et al. 2018). The pulse admixture model was set to the introgressed *Pungtius* species/population and its ancestral population pair based on phylogenomic and introgression detection. Specially, a single pulse admixture model was fitted to *P. laevis* and its ancestry population *P. pungitius*, and to *P. kaibarae* and its ancestry population *P. pungitius*, respectively; a double pulse admixture model was fitted to *P. sinensis* and its ancestry population *P. pungitius*, and to *Pungtius polyakovi* and its ancestry populations *P. pungitius* and *Pungtius tymensis*. The proportion of ancestry in the introgressed population was set to the admixture model based on *D*_{FOIL} tests abovementioned and estimation with Admixture (Alexander et al. 2009). The test was run with 1,000 bootstraps using a block size of 2,000 SNPs across the 20 autosomal LGs in the reference genome.

To infer the selection coefficient for fixation of adaptive introgression in *Pungtius* sticklebacks, simulations of the evolution in a 1-Mb genomic segment including introgression track were performed under a demographic model that considers three species/populations using SLiM 4.0.1 (Haller and Messer 2019). The selection coefficient(s) for the adaptive introgression varied between 0 and 1e−5, with mutation rate μ of 7.1×10^{-9} mutations per site as

estimated from Guo et al. (2013) and the recombination rate *r* of $1. \times 10^{-8}$ uniform across the segment as estimated below. For each selection coefficient value, 100 simulations were performed and 10 individuals for each population were sampled in each simulation. To reduce the computational burden of simulations, the simulation parameters were rescaled by a scaling factor *C*, where *C* = 10. The principle of scaling the parameter followed: population size = *N/C*, time = *t/C*, selection coefficient = *s* × *C*, mutation rate = $\mu \times C$, and recombination rate = *r* × *C*. Finally, discrete genomic segments with introgression signature in simulated individuals were identified using Ancestry-HMM. To identify the adaptive signal of introgression, the pattern of excess intermediate-frequency polymorphism produced in the flanking regions of the introgressed genomic region—a pattern that appears as a volcano-shape in pairwise genetic diversity—were scanned across the genome using VolcanoFinder (Setter et al. 2020).

Estimating Genome-wide Genetic Divergence

Genome-wide genetic parameters, nucleotide diversity (π), Tajima’s *D*, pairwise nucleotide divergence between species (*D*_{XY}; Nei 1987), and GC content were calculated across the reference genome with 100-kb nonoverlapping windows having at least 10 SNPs using VCFtools (Danecek et al. 2011), popgenWindows.py (https://github.com/simonhmartin/genomics_general), and bedtools (Quinlan and Hall 2010), respectively. Recombination rate across the reference genome in each species/population was estimated using LDhelmet (Chan et al. 2012). Genotypes were first phased across the reference genome

for the species/populations under study using BEAGLE (Browning and Browning 2009) with default parameters. Phased genotypes were further filtered and only those biallelic genotypes with a minimum genotype quality ≥ 30 and read depth between 10 and 100 were retained. Finally, the recombination map was estimated by running 1,000,000 Markov chain iterations with a burn-in of 100,000 iterations, a window size of 50 SNPs, block penalty of 50, and option of “pade” (-x 11) for Padé coefficient calculation in LDhelmet. The population level recombination rate was also estimated with LDhat (Auton and McVean 2007) by using unphased genotypes. The “interval” module in LDhat implemented a Bayesian MCMC sampling algorithm to estimate effective recombination rates across each chromosome in the reference genome. One million iterations were run with sampling once per 5,000 iterations and discarding the first 20% of samples as burn-in for each species/population. Recombination rates across the reference genome from LDhelmet and LDhat are highly consistent ($R \geq 0.72$, $P < 0.01$) in each species/population.

Demographic History Inference

The demographic history of *P. pungitius*, *P. kaibarae*, and *P. sinensis* in Northeast Asia (supplementary table S1, Supplementary Material online) was inferred using the pairwise sequential Markovian coalescence (PSMC) model (Li and Durbin 2011). An input file for PSMC was generated using the mpileup function in SAMtools (Li 2011) after read alignment with BWA as mentioned above, and minimum and maximum depth of coverage thresholds were set to twice and three times of the sample’s average coverage, respectively, using vcfutils. Heterozygous sites were detected from consensus sequences in FASTQ format using “fq2psmca” with a window size of 20 bp. PSMC was run with 20 iterations, an N0-scaled maximum coalescent time of 20, a ρ/θ ratio of 5, the 64-time intervals of “4 + 25 × 2 + 4 + 6,” and 100 bootstrap replicates. The generation time of 1 year (Ravinet et al. 2018) and mutation rate of $\mu = 7.1 \times 10^{-9}$ mutations per site per year were determined for *Pungitius* sticklebacks (Guo et al. 2013).

Reference Genome Annotation

Annotation of the *P. pungitius* reference genome was retrieved from Varadharajan et al. (2019). Conserved non-coding elements (CNEs) in the *P. pungitius* reference genome were identified as follows: Pairwise genome alignments between the *P. pungitius* and zebrafish (*Danio rerio*) genome (Zv9) were first done using LASTZ (Harris 2007). The lav files were then converted into psl format and chain together axt alignment using UCSC Genome Browser tools lavToPsl and axtChain. Next, newly detected repeat-overlapping alignments were incorporated into pairwise alignment chains using RepeatFiller (Osipova et al. 2019). Highly sensitive local pairwise alignment for loci flanked by aligning blocks was obtained using patchChain.perl (Hiller et al. 2013; Sharma and Hiller 2017), and the accuracy of local pairwise alignments was

improved using chainCleaner (Suarez et al. 2017). Finally, CNEs identified in the zebrafish genome (Hiller et al. 2013) were retrieved from GREAT (<http://great.stanford.edu/great/public/html/>), and their coordinate ranges in the zebrafish genome were converted into the *P. pungitius* genome using UCSC liftOver based on pairwise alignments between the two species’ genomes. Known and predicted protein–protein interactions in core gene regulatory networks underlying pelvic and lateral plate development were retrieved from STRING (<https://cn.string-db.org/>).

Results

Global Diversification of *Pungitius* Sticklebacks

Two divergent and strongly supported clades in *Pungitius* sticklebacks were identified based on genome-wide SNPs (fig. 1B), consistent with results of earlier studies (Takahashi et al. 2016; Guo et al. 2019; Wang et al. 2022). The *pungitius* clade split off from the *sinensis* clade 9.80 Ma (fig. 1C). The *pungitius* clade consisted of *Pungitius* sticklebacks from Europe, North America, and Asia, including *Pungitius platygaster* and *Pungitius hellenicus* from the Balkan Peninsula in southern Europe, *P. laevis* and *Pungitius vulgaris* from western Europe, and *P. pungitius* from North America, Asia, and Europe (fig. 1A and B). The *sinensis* clade consisted of *Pungitius* sticklebacks from northeast Asia, including *P. tymensis* from the islands of Sakhalin and Hokkaido, *Pungitius bussei* from Songhua River Basin, *P. kaibarae* from the Korean Peninsula, the Japanese archipelago, and Suifen-Khanka region, *P. sinensis* from the Japanese archipelago, the Russian Far East, and northeast China, as well as *P. polyakovi* from Sakhalin Island (fig. 1A and B). Despite the complex phylogeographic patterns, each currently recognized *Pungitius* species forms a monophyletic clade distinct from their sister species, except *P. polyakovi*, which falls within the *P. sinensis* clade forming a highly supported clade with *P. sinensis* from Sakhalin Island (fig. 1A and B). Armor traits (viz. lateral plates, pelvic apparatus, and keel) were indicated to have been repeatedly reduced in the course of evolution on both inter- and intraspecific levels (fig. 1B). For instance, lateral plate reduction was observed in *P. tymensis* that diverged from fully plated *P. bussei* and *P. kaibarae* 4.49 Ma, in *P. hellenicus* that diverged from fully plated *P. platygaster* 2.79 Ma, and in *P. sinensis* populations from the Japanese archipelago that diverged from fully plated *P. sinensis* populations from other geographic regions 1.05 Ma. No significant phylogenetic signal was detected in the reduction of lateral plates ($P \geq 0.27$), pelvic apparatus ($P \geq 0.46$), or caudal keel ($P \geq 0.48$) among the main *Pungitius* lineages based on either nuclear or mitochondrial phylogeny (fig. 1D).

Admixture Scenario in the Diversification of *Pungitius* Sticklebacks

Four cytonuclear discordances in the diversification of *Pungitius* sticklebacks (fig. 1D) were observed by

comparing the phylogenies inferred from genome-wide SNPs in this study and mitochondrial sequences from earlier studies (Wang et al. 2015, 2022; Takahashi et al. 2016; Guo et al. 2019). The four cytonuclear discordances involved all populations of *P. sinensis* and *P. polyakovi* and some populations of *P. kaibarae* and *P. laevis*, respectively. Introgression rather than ILS was detected in each of those four cytonuclear discordances with likelihood-based network tests based on thousands of genomic regions, with estimated inheritance probabilities ranging from 0.43 to 0.51 (supplementary table S2 and fig. S1, Supplementary Material online).

Frequent gene flow was detected between *Pungitius* species. Based on phylogeography, admixture between different *Pungitius* species was examined in 31 schemes involving 21 species pairs with a total of 644 Patterson's *D* tests (supplementary table S3, Supplementary Material online). Strong evidence for admixture was found in 22 schemes involving 15 *Pungitius* species pairs (supplementary table S3, Supplementary Material online; fig. 1D). *Pungitius pungitius* distributed across the northern hemisphere appeared in nine of the 22 admixture schemes, showing the most frequent gene flow with other *Pungitius* species. There was also a strong geographic component: 17 of the 22 admixture schemes involved *Pungitius* species/populations in Northeast Asia. Specifically, *P. pungitius* from the Far East had gene flow with all other *Pungitius* species in Northeast Asia except *P. bussei*. Gene flow between *Pungitius* species occurred in both range-wide populations (e.g., between *P. pungitius* and *P. sinensis*) and in specific populations (e.g., between from *P. polyakovi* and *P. tymensis* from Sakhalin Island). Extensive ancestral gene flow between *Pungitius* species was detected using D_{FOIL} statistics by including more species/populations in the testing phylogeny according to both admixture schemes from Patterson's *D* tests and phylogeography in *Pungitius* sticklebacks (supplementary table S4, Supplementary Material online; fig. 1D). The D_{FOIL} statistics also revealed that gene flow between *Pungitius* species in those admixture schemes detected with Patterson's *D* was bidirectional. Patterson's *D* test together with D_{FOIL} statistics showed that certain *Pungitius* species/populations were involved in multiple admixture events. For instance, *P. polyakovi* was involved in at least three admixture events, viz. the ancestral gene flow between *P. pungitius* and *P. sinensis*, the gene flow between *P. pungitius* from Far East and Sakhalin Island distributed *P. sinensis* and *P. polyakovi*, and the gene flow between *P. tymensis* and *P. polyakovi* (supplementary table S4, Supplementary Material online; fig. 1D). *Pungitius kaibarae* from the Japanese archipelago was involved in gene flow with *P. sinensis* and *P. tymensis* (supplementary table S4, Supplementary Material online; fig. 1D), respectively.

Genomic Landscape of Admixture

The genomic distribution of admixture signatures was quantified in six representative *Pungitius* species pairs

with bidirectional gene flow, including the four cases with cytonuclear discordances (fig. 2; supplementary figs. S2–S6 and table S5, Supplementary Material online). A consistent genomic signature of gene flow was observed in all six cases. Introgressions were highly asymmetric: in all six cases, more significant introgressions were detected from one *Pungitius* species to another (P3 to P2) than the other way round (P2 to P3) according to the D_{FOIL} statistics (fig. 2A; supplementary figs. S2A–S6A, Supplementary Material online). One species (P2 in the D_{FOIL} statistics) retained a larger number of introgressed genomic regions that are present across all chromosomes compared with another *Pungitius* species (P3 in the D_{FOIL} statistics) in each of the six cases (panels B–D in fig. 2 and supplementary figs. S2–S6 and table S6, Supplementary Material online). Many genes and CNEs were found in the introgressed genomic regions in one of the *Pungitius* species (P2 in the D_{FOIL} statistics) compared with another species (P3 in the D_{FOIL} statistics) in all six cases (panels E and F in fig. 2 and supplementary figs. S2–S6 and table S7, Supplementary Material online). The *Pungitius* species (P2 in the D_{FOIL} statistics) is thus hereinafter referred to as the recipient, and the species P3 in the D_{FOIL} statistics is the donor. Consistent genomic and population genetic features in introgressed genomic regions were observed compared with that in nonintrogressed genomic regions in the recipient species were observed. The introgressed genomic regions had a significantly lower recombination rate regardless of whether estimated with phased or unphased genotypes (Mann–Whitney *U* tests, $P < 3.8 \times 10^{-8}$), significantly higher nucleotide diversity (Mann–Whitney *U* tests, $P < 0.005$), and lower GC content in the reference genome compared with the nonintrogressed genomic regions in each recipient species (panels G–L in fig. 2 and supplementary figs. S2–S6, S7A, Supplementary Material online). The introgressed genomic regions had lower absolute population divergence with other species compared with the nonintrogressed genomic regions in each recipient species (panels a and c in supplementary fig. S8A–F, Supplementary Material online). The tree topology based on SNPs in the introgressed genomic regions switches from a “species tree” to an “introgression tree” in each recipient species (panels b and d in supplementary fig. S8A–F, Supplementary Material online). The introgressive genomic regions had a significantly higher recombination rate (Mann–Whitney *U* tests, $P < 0.008$) and significantly higher nucleotide diversity (Mann–Whitney *U* tests, $P < 0.04$) compared with nonintrogressive genomic regions in each donor species (supplementary fig. S7B–D, Supplementary Material online).

Ancestry tracks in each individual genome were inferred in the four cases involving cytonuclear discordances (supplementary fig. S9, Supplementary Material online). Recent admixture pulse was identified in the recipient *P. laevis* from its donor *P. pungitius* (left panel, supplementary fig. S9A, Supplementary Material online) and in the recipient *P. polyakovi* from its donor *P. tymensis*

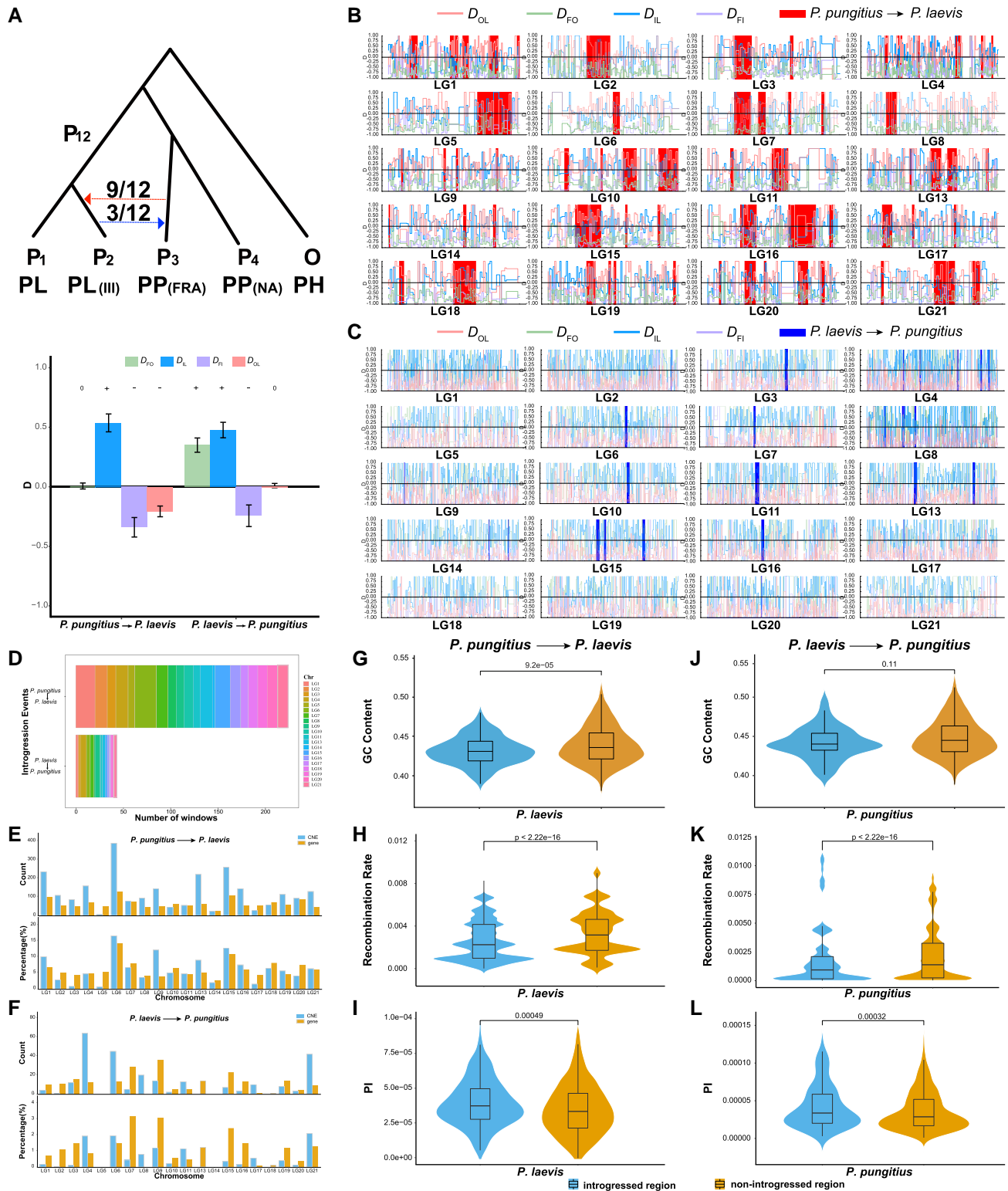


FIG. 2. The genomic landscape of admixture signatures between *Pungitius pungitius* and *Pungitius laevis*. (A) Top panel: Number of total tests (after slash) and significant introgressions (before slash) detected between *P. pungitius* and *P. laevis* with D_{FOIL} statistics. Bottom panel: Expected signs of the D_{FOIL} statistics components (D_{FO} , D_{IL} , D_{FI} , and D_{OL}) for gene flow from *P. pungitius* to *P. laevis* (0/+/-/-) and from *P. laevis* to *P. pungitius* (+/+/-/-), which is adopted from Pease and Hahn (2015). (B and C) Genome-wide distribution of genomic regions with introgression signatures in *P. laevis* and *P. pungitius*. The red bars mark genomic regions in *P. laevis* with gene flow from *P. pungitius* to *P. laevis*, and the blue bars mark genomic regions in *P. pungitius* with gene flow from *P. laevis* to *P. pungitius*. Lines are genome-wide distribution of D_{FOIL} statistics. (D) Number of genomic regions with introgression signatures in each chromosome in *P. laevis* (top panel) and *P. pungitius* (bottom panel). Number of genes and CNEs located in genomic regions with introgression signatures and their proportions accounting for total number of genes and CNEs in each chromosome in *P. laevis* (E) and in *P. pungitius* (F). Comparison of GC content, recombination rate, and nucleotide diversity between introgressed and nonintrogressed genomic regions in *P. laevis* (G–I) and in *P. pungitius* (J–L). Numbers are P -values from Mann–Whitney U tests.

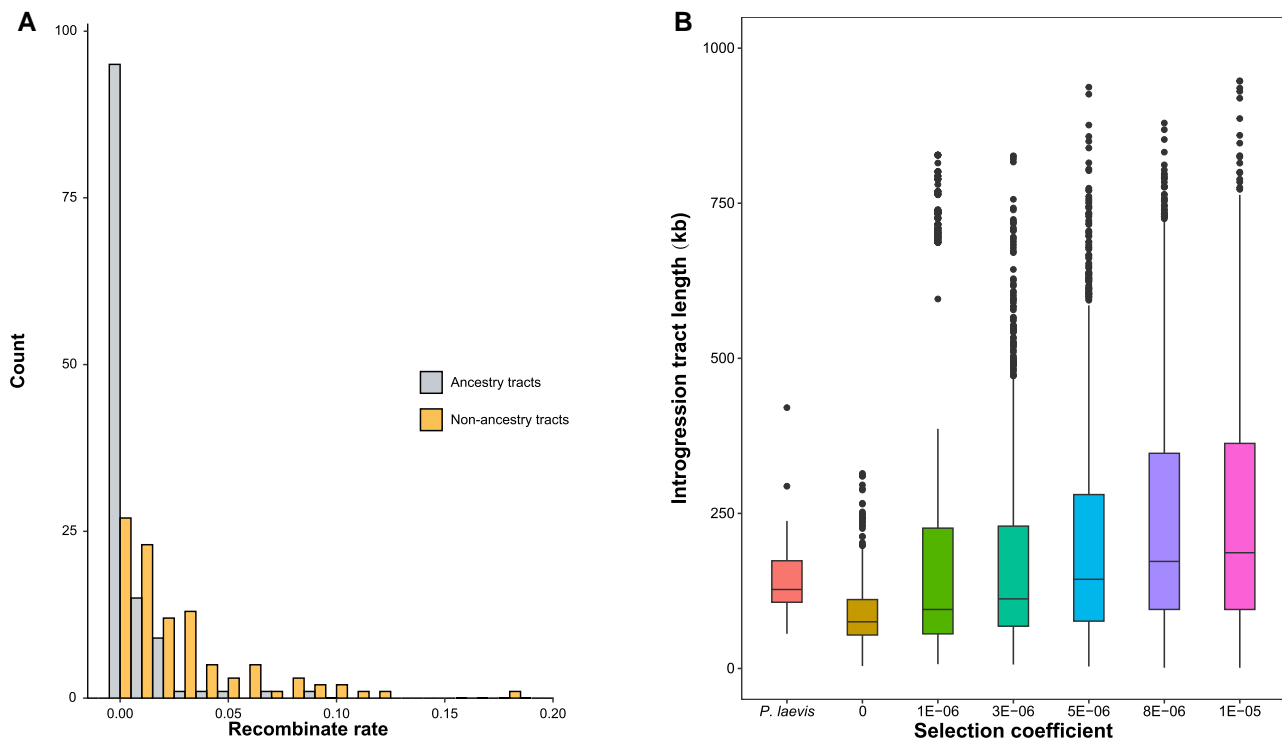


FIG. 3. Features of ancestry tracts identified with Ancestry_HMM in the recipient *Pungitius laevis* population. (A) Comparison of recombination rate in the 172 genomic regions between individual with ancestry tract and individual without ancestry tract. Recombination rates estimated by LDhelmet were converted into rates in 100-kb nonoverlapping windows. (B) Length of ancestry tracts inferred from 12 individuals in the recipient *P. laevis* population and relationship between introgressed genomic tract length and selection coefficient with simulations. Each data point in the box plot represents the length of an introgressed genomic tract identified in empirical and simulation data.

(left panel, [supplementary fig. S9B, Supplementary Material](#) online). Accordingly, a total of 172 ancestry tracks were identified in 12 of *P. laevis* individuals (right panel, [supplementary fig. S9A, Supplementary Material](#) online) and 142 in 4 of *P. polyakovi* individuals (right panel, [supplementary fig. S9B, Supplementary Material](#) online). Relatively ancient admixture pulse was found in the recipient *P. polyakovi* from its donor *P. pungitius*, in the recipient *P. sinensis* from its donor *P. pungitius*, and in the recipient *P. kaibarae* from its donor *P. pungitius* (left panel, [supplementary fig. S9B–D, Supplementary Material](#) online). As such, a few ancestry tracks were identified in the recipient individual genomes (right panel, [supplementary fig. S9B–D, Supplementary Material](#) online). It is worth noting that all ancestry tracks identified with Ancestry_HMM overlap the introgressed regions identified with D_{FOIL} statistics. In the recipient *P. laevis*, the length of the 172 ancestry tracts ranged from 55 to 420 kb, and recombination rate in the 172 genomic regions in individual with ancestry tract was significantly lower than that in individual without ancestry tract (Wilcoxon signed-rank test, $P < 2.4 \times 10^{-16}$; [fig. 3](#)). To infer the selection coefficients from admixture to selection, simulations were performed by considering the genome-wide pattern of introgression genomic tracks in the recipient *P. laevis* population, since the introgression occurred recently according to Ancestry_HMM analysis and

population level genome-wide data were available. Three populations representing *P. pungitius*, the ancestral population of *P. laevis*, and *P. vulgaris* were simulated based on their demography ([supplementary fig. S10, Supplementary Material](#) online). By directly tracking the introgressed segments from 1,000 individuals from simulation, a positive correlation between introgressed tract length and the selection coefficients is found, and the selection coefficient for the current length distribution of ancestry tracts in the recipient *P. laevis* population was estimated between 3×10^{-6} and 5×10^{-6} ([fig. 3B](#)).

Footprints of Introgression in the Core Gene Regulatory Network of Armor Trait Development

The recipient species/populations had similar armor traits (viz. lateral plate and pelvic phenotypes) as the donor species/populations in the four cases involving cytonuclear discordances ([supplementary table S8, Supplementary Material](#) online). To assess the potential genetic impact of introgression in the convergent phenotypic evolution in *Pungitius* sticklebacks, the footprint of introgression in the core gene regulatory network of armor trait development was thoroughly characterized in these four cases ([figs. 4 and 5; supplementary figs. S12–S17, Supplementary Material](#) online). Genes in the core gene regulatory network of armor trait development ([figs. 4A](#)

and 5A; supplementary figs. S12A–S17A, Supplementary Material online) are significantly more frequently located in genomic regions with admixture signatures than genome-wide genes (supplementary table S7, Supplementary Material online) in the recipient species/populations (viz. *P. laevis*, *P. polyakovi*, and *P. kaibarae*; Yates-corrected χ^2 tests, $P < 0.02$), with the exception of *P. sinensis* (Yates-corrected χ^2 tests, $P > 0.18$). In addition to these genes, their potential *cis*-regulatory regions (CNEs) are frequently located in genomic regions with admixture signatures, including *mapk8b* and *msx2a* in the core gene regulatory network of lateral plate development (fig. 4), and *BMP4*, *tbx5a*, and *egr1* in the core gene regulatory network of pelvic development (fig. 5) in the recipient *P. laevis* population. This is also observed in the recipient *P. sinensis* (supplementary figs. S12 and S13, Supplementary Material online), *P. kaibarae* (supplementary figs. S14 and S15, Supplementary Material online), and *P. polyakovi* (supplementary figs. S16 and S17, Supplementary Material online) populations. Genomic regions with genes *mapk8b* and *msx2a* in the core gene regulatory network of lateral plate development (supplementary figs. S4, S12, S14, and S16, Supplementary Material online) and the gene *BMP4* in the core gene regulatory network of pelvic development (fig. 5, supplementary figs. S13, S15, and S17, Supplementary Material online) were found to show admixture signatures repeatedly in all four cases where cytonuclear discordances occurred. The introgressed genomic regions with genes in the core gene regulatory network of armor trait development had positive Tajima's *D* values in the recipient *P. laevis* population, but negative Tajima's *D* values in nonrecipient species/populations (figs. 4 and 5). Genome scans with VolcanoFinder revealed that introgressed genomic regions with genes in the core gene regulatory network of armor trait development commonly had large likelihood ratios (figs. 4 and 5). Positive Tajima's *D* values and large likelihood ratios from genome scans were also observed in the introgressed genomic regions with genes in the core gene regulatory network of armor trait development in other recipient species/populations. These included, for instance, introgressed genomic regions with genes *wnt8b* and *lhx4* in the recipient *P. sinensis* population (supplementary fig. S13, Supplementary Material online), *edaradd*, *lhx4*, and *wnt8b* in the recipient *P. kaibarae* population (supplementary figs. S14 and S15, Supplementary Material online), and *msx2a* in the recipient *P. polyakovi* population (supplementary fig. S16, Supplementary Material online). With additional genotyping in both donor and recipient populations not only the genotyping accuracy but also alleles with admixture signature is confirmed. Examples of these include SNP at position of 9365057 in LG 6 near *mapk8b* gene (fig. 4) and SNPs at positions of 33046989 and 33046991 in LG 6 near *egr1* gene (fig. 5) in the recipient *P. laevis* population and the donor *P. pungitius* population from West Europe. The same pattern is also observed in other *Pungitius* pairs with gene flow (supplementary figs. S12–S17, Supplementary Material online).

Discussion

Genomic data have revealed that introgression is prevalent and frequently promotes adaptation and diversification in nature (Arnold and Kunte 2017; Taylor and Larson 2019; Edelman and Mallet 2021). Using genome-wide SNP data from a comprehensive sampling of *Pungitius* sticklebacks, our results demonstrate that introgression is widespread in this genus, and is frequently associated with their adaptive diversification. Although gene flow was found to be bidirectional, introgression was consistently asymmetric and left unequal genomic signatures in the species investigated. More significantly, in cases where asymmetric introgression was observed, the direction of stronger introgression appeared to be accompanied by phenotype transfer from one species to another. Genomic regions with genes in the core gene regulatory network of armor trait development in the recipient population frequently showed signatures of adaptive introgression, suggesting that introgression may be an important source of adaptive variation underlying phenotypic convergence in *Pungitius* sticklebacks. In the following, we discuss the significance of these findings in light of the generality of introgression in evolution and genetic mechanisms underlying convergence in sticklebacks.

Prevalent and Biased Introgression in the Diversification of *Pungitius* Sticklebacks

The extent of genetic exchange between divergent evolutionary lineages in nature is a topic of broad interest in contemporary evolutionary biology (Taylor and Larson 2019; Edelman and Mallet 2021). Systematic investigation of introgression in entire evolutionary clades can aid our understanding of introgression generality and specificity across the tree of life (Pease et al. 2016; Malinsky et al. 2018; Edelman et al. 2019; Vanderpool et al. 2020; Suvorov et al. 2022). Using genome-scale sequence data, we provided a systematic survey of introgression events across the phylogeny of *Pungitius* sticklebacks. We first find that at least 22 pairs of lineages have experienced ancient and/or recent introgression across the *Pungitius* phylogeny, and only one (*P. bussei*) of the 10 studied *Pungitius* species has not had recent gene flow with other species (supplementary table S3, Supplementary Material online; fig. 1D). Our results thus show that introgression has occurred more frequently than suggested by earlier studies (Takahashi and Takata 2000; Takahashi et al. 2003, 2016; Tsuruta and Goto 2006; Wang et al. 2015, 2017, 2022; Guo et al. 2019; Yamasaki et al. 2020) in the diversification of *Pungitius* sticklebacks.

In addition to providing an estimate of the number of introgression events, our results are informative about the chronology of introgression, which is the key to understanding the complex cytonuclear discordance in *Pungitius* sticklebacks, especially when a lineage has experienced multiple independent introgression events. Consistent with the results of an earlier study using genome-wide sequence data (Wang et al. 2022), *P. polyakovi* from its type

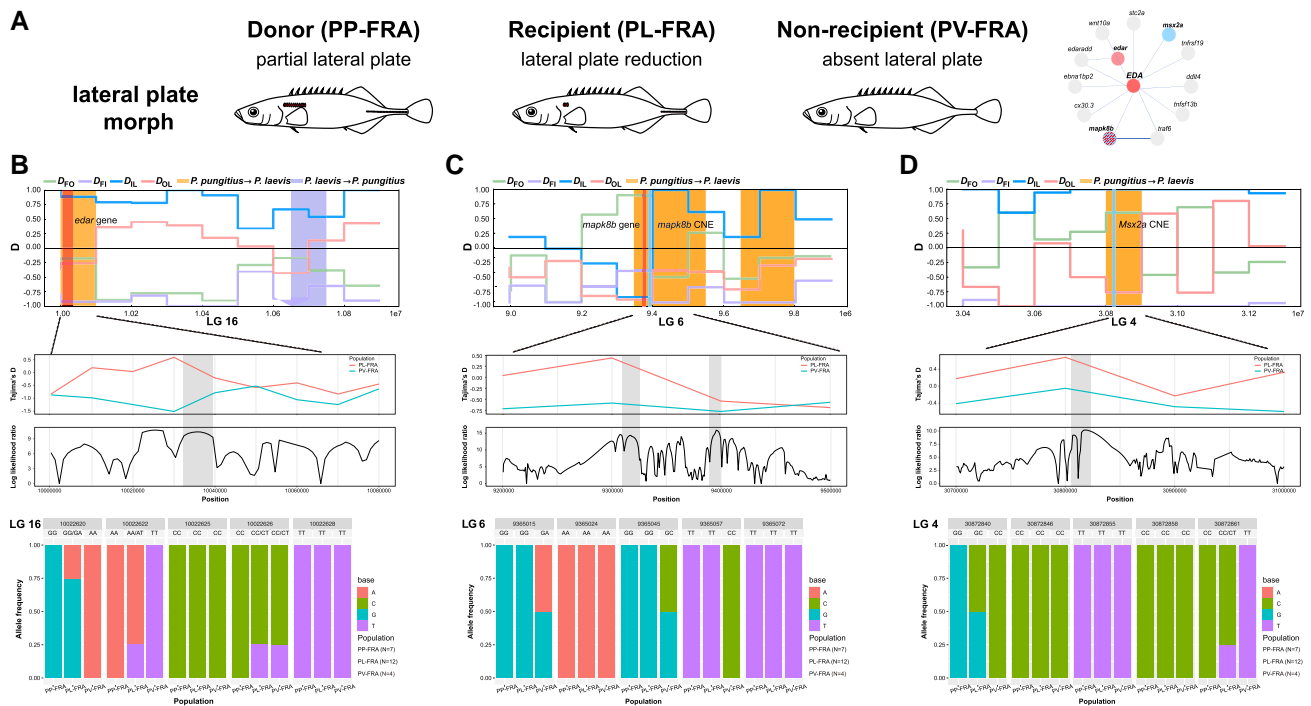


Fig. 4. The footprint of introgression in core gene regulatory network of lateral plate development in the recipient *Pungitius laevis* population. (A) Lateral plate morph in donor (*Pungitius pungitius*, PP-FRA), recipient (*P. laevis*, PL-FRA), and nonrecipient population (*Pungitius vulgaris*, PV-FRA) from western Europe, and core gene regulatory network of lateral plate development. Introgression signatures in the recipient population (top panel), Tajima's *D* in the recipient and nonrecipient population and maximum likelihood test statistic of adaptive introgression in the recipient population (middle panel), and allele frequencies of SNPs in donor, recipient, and nonrecipient population (bottom panel) in genomic regions with genes (B) *edar*, (C) *mapk8b*, and (D) *msx2a*.

locality forms a well-supported clade with *P. sinensis* from Sakhalin Island (fig. 1B); however, when analyzed with mitochondrial data, it forms a clade with *P. tymensis* (Takahashi et al. 2016). The most parsimonious explanation for this cytonuclear discordance is that the mitogenome of *P. polyakovi* has been first replaced by a *P. pungitius*-type mitogenome after *P. pungitius* diverged from *P. laevis* (3.47 Ma) and before the diversification of *P. sinensis* (1.05 Ma), and then became replaced by a *P. tymensis*-type mitogenome (0.14 Ma) after the divergence between *P. tymensis* populations from Sakhalin Island and the Japanese archipelago (fig. 1C and D). Our results indeed show that *P. polyakovi* and *P. sinensis* have experienced ancient gene flow with *P. pungitius* and recent gene flow with *P. tymensis* (fig. 1D; supplementary tables S4 and S5, Supplementary Material online), which is also supported by the local ancestry inference in the *P. polyakovi* population (supplementary fig. S9B, Supplementary Material online). This indicates that *P. polyakovi* is actually a *P. sinensis* population that had gene flow with *P. tymensis*. Likewise, multiple independent introgression events were observed in *P. sinensis* with *P. pungitius*. The mitogenome of the ancestral *P. sinensis* became replaced with the *P. pungitius*-type mitogenome 3.47–1.05 Ma in an ancient introgression event (Wang et al. 2015, 2022; Takahashi et al. 2016; Guo et al. 2019), and *P. sinensis* and *P. pungitius* from the Japanese archipelago came into secondary contact 0.59–0.21 Ma (fig. 1C and D) or later (Yamasaki et al. 2020).

Our results show that introgression left detectable signals within the extant genomes of *Pungitius* sticklebacks according to *D* statistics (fig. 2; supplementary figs. S2–S8, Supplementary Material online), and ancestry tracts in recipient populations in which introgression occurred recently were clearly traceable (supplementary fig. S9, Supplementary Material online). Genomic signatures of introgression were consistently unequal between the recipient and donor populations (supplementary tables S6 and S7, Supplementary Material online), although gene flow was commonly bidirectional. In fact, although unequal introgression between the recipient and donor population is commonly observed, little is known about how ecological, behavioral, and evolutionary factors determine which genetic variation moves between species, whether such factors bias gene flow from one species to another, and whether any such biases affect how genetic variation from one species is ultimately retained in the genome of the other (Pfennig 2021). The occurrence of introgression requires that hybrids interbreed with at least one of the parental species. However, mating between species is often not random (Rosenthal 2013; Willis 2013), as observed in *Pungitius* sticklebacks in common garden experiments (supplementary table S9, Supplementary Material online; Natri et al. 2019). Survival rate to the adult stage of hybrids in crosses between *P. sinensis* males and *P. pungitius* females is clearly different from that of hybrids between *P. sinensis* females and *P. pungitius* males (Natri

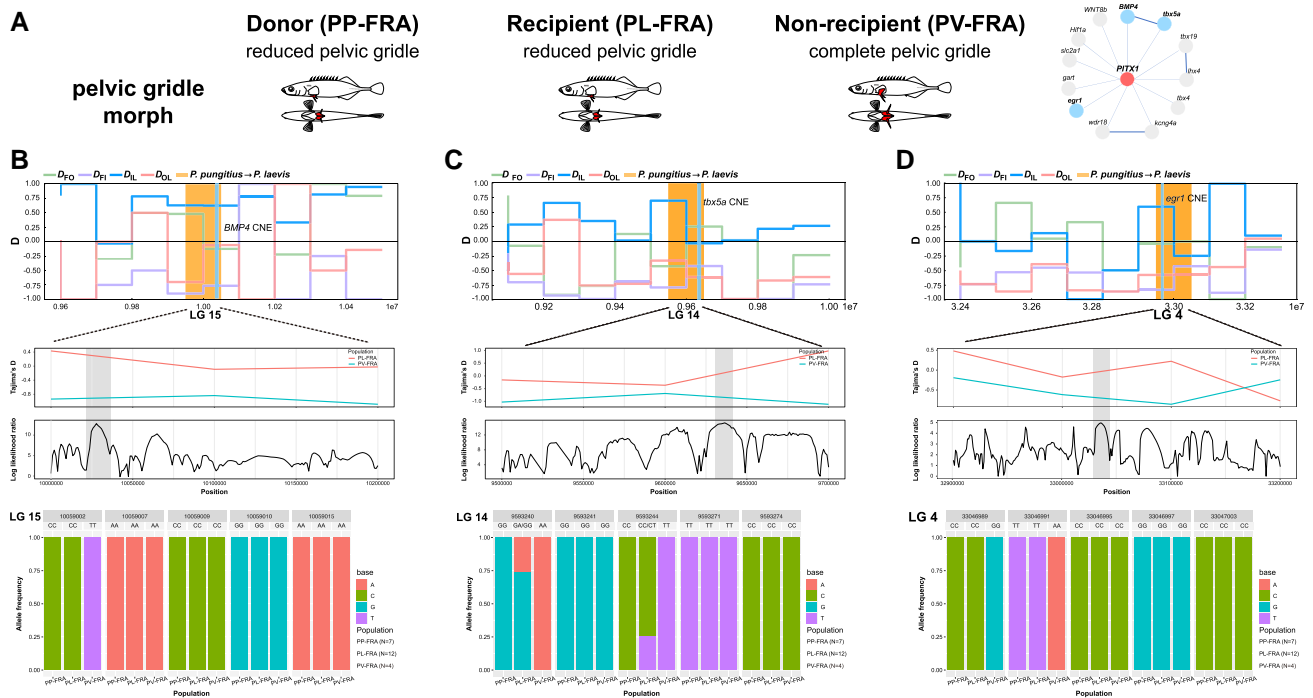


FIG. 5. The footprint of introgression in core gene regulatory network of pelvic development in the recipient *Pungitius laevis* population. (A) Pelvic morph in donor (*Pungitius pungitius*, PP-FRA), recipient (*P. laevis*, PL-FRA), and nonrecipient population (*Pungitius vulgaris*, PV-FRA) from western Europe, and core gene regulatory network of pelvic development. Introgression signatures in the recipient population (top panel), Tajima's *D* in the recipient and nonrecipient population and maximum likelihood test statistic of adaptive introgression in the recipient population (middle panel), and allele frequencies of SNPs in donor, recipient, and nonrecipient population (bottom panel) in genomic regions with genes (B) *BMP4*, (C) *tbx5a*, and (D) *egr1*.

et al. 2019). This phenomenon is also seen in crosses of *P. kaibarae* with *P. pungitius* (Natri et al. 2019). Thus, the gene flow between *Pungitius* species consists of a nonrandom sample of the segregating variation in hybrids.

Once introgression occurs, the genomic landscape of introgression between species is shaped by differential fitness effects of introgressed variants across the genome, and fixation of the introgressed variation requires either long time periods, small population sizes, or selection on the introgressed region (Arnold and Kunte 2017; Martin and Jiggins 2017). Since selection is less effective in fixing (or removing) introgressed variation in the genomes of smaller populations, differences in effective population sizes can lead to a strong variation in admixture proportions among populations (Sankararaman et al. 2014). Population size may thus be particularly relevant for unequal introgression between the recipient and donor population in *Pungitius* sticklebacks, since these populations are known to be small in general (Merilä 2013; Bae and Suk 2015; Kemppainen et al. 2021; Feng et al. 2022). In this study, the recipient populations (e.g., *P. sinensis* and *P. kaibarae* from the Japanese archipelago) have much smaller population sizes than the donor populations (e.g., *P. pungitius* from the Japanese archipelago; supplementary fig. S11, Supplementary Material online; Yamasaki et al. 2020). Thus, the unequal admixture signatures between species could be, at least partly, due to

biased hybridization and/or differences in population size between donor and recipient populations.

Introgression Underlying Convergence in *Pungitius* Sticklebacks

The signals of introgression across the *Pungitius* phylogeny and genomes provides evidence for widespread introgression, yet the evolutionary significance of this introgression in the diversification of *Pungitius* sticklebacks has been poorly understood. Sticklebacks are well known for repeated reduction of armor traits when adapting to freshwater (Bell and Foster 1994; Peichel and Marques 2017); in three-spined sticklebacks, this phenomenon is thought to be due to a trade-off between armor and growth, as growth rate of heavily armored individuals with genotypes for complete armor is reduced. Given the importance of growth for overall fitness, the genotype for reduced armor is favored in freshwater environments (Barrett 2010). However, our analysis shows that armor traits in *Pungitius* sticklebacks show repeated losses and gains across their phylogeny and are poor indicators of phylogenetic relationships in this genus, which likely explains the difficulties in establishing robust *Pungitius* taxonomy (Guo et al. 2019).

Our results further show that asymmetric introgression is strongly associated with corresponding phenotypic transitions from the donor to the recipient in *Pungitius*

sticklebacks (supplementary table S8, Supplementary Material online). The four cytonuclear discordances are cases in point: the results show that they have experienced introgression, and the recipient species/populations have preserved much more of the introgressed variation than the donor populations. It is known that introgression can shape trait evolution in both animals and plants, and can generate apparently convergent patterns of evolution (Lamichaney et al. 2015; Zhang et al. 2016; Jones et al. 2018; Giska et al. 2019; Gibson et al. 2021). To explore the possible role of introgression in the phenotype transfer in *Pungitius* sticklebacks, we investigated introgression signatures in the core gene regulatory networks of armor trait development in the recipient populations. In the core gene regulatory network of lateral plate development, the homeobox-containing transcription factor in skeletal development (*Msx2a*) is a major gene underlying dorsal spine reduction in freshwater three-spined sticklebacks (Howes et al. 2017), whereas *Stc2a* is a secreted glycoprotein with autocrine or paracrine functions and a potent inhibitor of bone growth (Gagliardi et al. 2005). The *Msx2a-Stc2a* region maps 1.1 Mb from *Eda*, the major locus of armor plating in three-spined stickleback (Kingman et al. 2021). *Msx2a* is associated with the *Eda* gene controlling bony plate loss, which helps to explain the concerted effects of chrIV on multiple armor reduction traits. In the core gene regulatory network of pelvic development, *Wnt8b* and *Tbx4* downstream of *Pitx1* are involved in pelvic fin/hindlimb development (Don et al. 2013) and hindlimb development (Tickle and Cole 2004), respectively. It has been shown that knockout of *Tbx4* in zebrafish can result in reduction of pelvic fins (Lin et al. 2016). Our results show that introgression signatures are extensively found in genomic regions with these genes and/or their CNEs (figs. 4 and 5; supplementary figs. S12–S17, Supplementary Material online). Extensive simulations show that genome-wide introgressed variants in recipient *Pungitius* populations are not fixed randomly in terms of the ancestry tracts length (fig. 3B). Signatures of positive selection and adaptive sweeps in the putatively introgressed regions with those genes were found according to Tajima's *D* and likelihood ratios from VolcanoFinder, respectively, suggesting that fixation of introgressed variation in those cases is adaptive. Therefore, introgression might play an important role in generating genetic parallelism underlying phenotypic convergence in *Pungitius* sticklebacks. Notably, in addition to armor trait convergence, introgression might also underly the evolution of sex chromosomes in *Pungitius* sticklebacks. The Y chromosome in *P. pungitius* was found to be established by ancient introgression with *P. sinensis* (Dixon et al. 2019; Natri et al. 2019), highlighting the diverse impacts of introgression on evolution.

Conclusions

Our results demonstrate that introgression in the diversification of *Pungitius* sticklebacks is much more prevalent

than earlier studies suggested. Although this introgression has been bi-directional, it has left highly asymmetric genomic signatures in the genomes of hybridizing species. The results further demonstrate that some of the introgressed elements have fueled adaptation. In several instances, introgression of the core genes in regulatory networks coding armor trait development from one species to another were accompanied by corresponding phenotypic transitions from one species to another. This suggests that introgression may have been an important source of adaptive variation underlying phenotypic convergence and divergence in *Pungitius* sticklebacks. Furthermore, this introgression-driven convergence likely explains the longstanding difficulties in resolving the taxonomy and systematics of this small but phenotypically highly diverse group of fish.

Supplementary material

Supplementary data are available at *Molecular Biology and Evolution* online.

Acknowledgments

The authors thank Victor Berger, Chunguang Zhang, Chris Eberlein, Abigel Gonda, Akira Goto, Shunping He, Gábor Herczeg, Kjetill Hindar, Takefumi Kitamura, Nellie Konijnendijk, Jennyfer Lacasse, Dmitry Lajus, Vladimir Loginov, Scott McCairns, Heini Natri, Ola Ugedahl, Henri Persat, Tom Pike, Joost Raeymaekers, Beren Robinson, Radek Sanda, Garrett Staines, Mark Steinhilber, Haibo Liu, Chengyi Niu, Dandan Qi, Frank A. von Hippel, people at the Oulanka Research Station in Finland, and the China National Animal Collection Resource Center (<http://museum.ioz.ac.cn/>) for help in fish sampling, Kirsi Kähkönen and Miinastiina Issakainen for help in DNA extraction, and editors, Sophie von der Heyden and Matthew Hahn, and two anonymous reviewers for constructive comments in revision. The work was funded by the National Natural Science Foundation of China (Grant Nos. 32161160321, 31672273, and 32022009), the Academy of Finland (Grant Nos. 129662, 134728, and 218343), a grant from the NSFC/RGC Joint Research Scheme sponsored by the Research Grants Council of the Hong Kong Special Administrative Region, China, and the National Natural Science Foundation of China (Project No. N_HKU763/21), and the Chinese Academy of Sciences (ZDBS-LY-SM005 and the Pioneer Hundred Talents Program).

Author Contributions

B.G. conceived this study. Yu.W., Yi.W., X.C., Y.D., and C.W. performed analyses. B.G., Yu.W., and J.M. wrote the manuscript. B.G. and J.M. contributed to funding acquisition. All authors commented on the manuscript.

Data Availability

Sequence data generated in this study is deposited in GenBank, and accession numbers for all involved sequencing data are listed in [supplementary table S1, Supplementary Material](#) online.

References

- Alexander DH, Novembre J, Lange K. 2009. Fast model-based estimation of ancestry in unrelated individuals. *Genome Res.* **19**: 1655–1664.
- Arnold ML, Kunte K. 2017. Adaptive genetic exchange: a tangled history of admixture and evolutionary innovation. *Trends Ecol Evol (Amst)*. **32**:601–611.
- Auton A, McVean G. 2007. Recombination rate estimation in the presence of hotspots. *Genome Res.* **17**:1219–1227.
- Bae HG, Suk HY. 2015. Population genetic structure and colonization history of short ninespine sticklebacks (*Pungitius kaibarae*). *Ecol Evol.* **5**:3075–3089.
- Barrett RDH, Schluter D. 2008. Adaptation from standing genetic variation. *Trends Ecol Evol (Amst)*. **23**:38–44.
- Barrett RDH. 2010. Adaptive evolution of lateral plates in three-spined stickleback *Gasterosteus aculeatus*: a case study in functional analysis of natural variation. *J Fish Biol.* **77**:311–328.
- Bell MA, Foster SA. 1994. *The evolutionary biology of the threespine stickleback*. Oxford: Oxford University Press
- Bouckaert R, Heled J, Kuhnert D, Vaughan T, Wu CH, Xie D, Suchard MA, Rambaut A, Drummond AJ. 2014. BEAST 2: a software platform for Bayesian evolutionary analysis. *PLoS Comput Biol.* **10**: e1003537.
- Browning BL, Browning SR. 2009. A unified approach to genotype imputation and haplotype-phase inference for large data sets of trios and unrelated individuals. *Am J Hum Genet.* **84**:210–223.
- Bryant D, Bouckaert R, Felsenstein J, Rosenberg NA, RoyChoudhury A. 2012. Inferring species trees directly from biallelic genetic markers: bypassing gene trees in a full coalescent analysis. *Mol Biol Evol.* **29**:1917–1932.
- Burgarella C, Barnaud A, Kane NA, Jankowski F, Scarcelli N, Billot C, Vigouroux Y, Berthouly-Salazar C. 2019. Adaptive introgression: an untapped evolutionary mechanism for crop adaptation. *Front Plant Sci.* **10**:4.
- Chan AH, Jenkins PA, Song YS. 2012. Genome-wide fine-scale recombination rate variation in drosophila melanogaster. *PLoS Genet.* **8**: e1003090.
- Chan YF, Marks ME, Jones FC, Villarreal G, Shapiro MD, Brady SD, Southwick AM, Absher DM, Grimwood J, Schmutz J, et al. 2010. Adaptive evolution of pelvic reduction in sticklebacks by recurrent deletion of a *Pitx1* enhancer. *Science* **327**:302–305.
- Colosimo PF, Hosemann KE, Balabhadra S, Villarreal G, Dickson M, Grimwood J, Schmutz J, Myers RM, Schluter D, Kingsley DM. 2005. Widespread parallel evolution in sticklebacks by repeated fixation of ectodysplasin alleles. *Science* **307**:1928–1933.
- Colosimo PF, Peichel CL, Nereng K, Blackman BK, Shapiro MD, Schluter D, Kingsley DM. 2004. The genetic architecture of parallel armor plate reduction in threespine sticklebacks. *PLoS Biol.* **2**:635–641.
- Cresko WA, Amores A, Wilson C, Murphy J, Currey M, Phillips P, Bell MA, Kimmel CB, Postlethwait JH. 2004. Parallel genetic basis for repeated evolution of armor loss in Alaskan threespine stickleback populations. *Proc Natl Acad Sci U S A.* **101**:6050–6055.
- Danecek P, Auton A, Abecasis G, Albers CA, Banks E, DePristo MA, Handsaker RE, Lunter G, Marth GT, Sherry ST, et al. 2011. The variant call format and VCFtools. *Bioinformatics* **27**:2156–2158.
- Darwin C. 1859. *On the origin of species by means of natural selection, or the preservation of favoured races in the struggle for life*. London: J. Murray. p. 502.
- Denys GPJ, Persat H, Dettai A, Geiger MF, Freyhof J, Fesquet J, Keith P. 2018. Genetic and morphological discrimination of three species of ninespined stickleback *Pungitius* spp. (Teleostei, Gasterosteidae) in France with the revalidation of *Pungitius vulgaris* (Mauduyt, 1848). *J Zool Syst Evol Res.* **56**:77–101.
- Dixon G, Kitano J, Kirkpatrick M. 2019. The origin of a new sex chromosome by introgression between two stickleback fishes. *Mol Biol Evol.* **36**:28–38.
- Don EK, Currie PD, Cole NJ. 2013. The evolutionary history of the development of the pelvic fin/hindlimb. *J Anat.* **222**:114–133.
- Durand EY, Patterson N, Reich D, Slatkin M. 2011. Testing for ancient admixture between closely related populations. *Mol Biol Evol.* **28**: 2239–2252.
- Edelman NB, Frandsen PB, Miyagi M, Clavijo B, Davey J, Dikow RB, Garcia-Accinelli G, Van Belleghem SM, Patterson N, Neafsey DE, et al. 2019. Genomic architecture and introgression shape a butterfly radiation. *Science* **366**:594–599.
- Edelman NB, Mallet J. 2021. Prevalence and adaptive impact of introgression. *Annu Rev Genet.* **55**:265–283.
- Fang B, Kempainen P, Momigliano P, Feng XY, Merilä J. 2020. On the causes of geographically heterogeneous parallel evolution in sticklebacks. *Nat Ecol Evol.* **4**:1105–1115.
- Feng XY, Merilä J, Löytynoja A. 2022. Complex population history affects admixture analyses in nine-spined sticklebacks. *Mol Ecol.* **31**: 5386–5401.
- Fritz SA, Purvis A. 2010. Selectivity in mammalian extinction risk and threat types: a new measure of phylogenetic signal strength in binary traits. *Conserv Biol.* **24**:1042–1051.
- Gagliardi AD, Kuo EYW, Raulic S, Wagner GF, DiMattia GE. 2005. Human stanniocalcin-2 exhibits potent growth-suppressive properties in transgenic mice independently of growth hormone and IGFs. *Am J Physiol Endocrinol Metab.* **288**:E92–E105.
- Gibson G. 2005. The synthesis and evolution of a supermodel. *Science* **307**:1890–1891.
- Gibson MJS, Torres MD, Brandvain Y, Moyle LC. 2021. Introgression shapes fruit color convergence in invasive Galapagos tomato. *Elife* **10**:e64165.
- Giska I, Farello L, Pimenta J, Seixas FA, Ferreira MS, Marques JP, Miranda I, Letty J, Jenny H, Hacklander K, et al. 2019. Introgression drives repeated evolution of winter coat color polymorphism in hares. *Proc Natl Acad Sci U S A.* **116**:24150–24156.
- Guo B, Chain FJJ, Bornberg-Bauer E, Leder EH, Merilä J. 2013. Genomic divergence between nine- and three-spined sticklebacks. *BMC Genomics.* **14**:756.
- Guo B, Fang B, Shikano T, Momigliano P, Wang C, Kravchenko A, Merilä J. 2019. A phylogenomic perspective on diversity, hybridization and evolutionary affinities in the stickleback genus *Pungitius*. *Mol Ecol.* **28**:4046–4064.
- Haller BC, Messer PW. 2019. SLim 3: forward genetic simulations beyond the wright–fisher model. *Mol Biol Evol.* **36**:632–637.
- Harris RS. 2007. *Improved pairwise alignment of genomic DNA*. State College (PA): The Pennsylvania State University.
- Hedrick PW. 2013. Adaptive introgression in animals: examples and comparison to new mutation and standing variation as sources of adaptive variation. *Mol Ecol.* **22**:4606–4618.
- Hendry AP, Peichel CL, Matthews B, Boughman JW, Nosil P. 2013. Stickleback research: the now and the next. *Evol Ecol Res.* **15**: 111–141.
- Hiller M, Agarwal S, Notwell JH, Parikh R, Guturu H, Wenger AM, Bejerano G. 2013. Computational methods to detect conserved non-genic elements in phylogenetically isolated genomes: application to zebrafish. *Nucleic Acids Res.* **41**:e151–e151.
- Hohenlohe PA, Bassham S, Etter PD, Stiffler N, Johnson EA, Cresko WA. 2010. Population genomics of parallel adaptation in threespine stickleback using sequenced RAD tags. *PLoS Genet.* **6**: e1000862.
- Howes TR, Summers BR, Kingsley DM. 2017. Dorsal spine evolution in threespine sticklebacks via a splicing change in *MSX2A*. *BMC Biol.* **15**:1–16.

- Ishikawa A, Takeuchi N, Kusakabe M, Kume M, Mori S, Takahashi H, Kitano J. 2013. Speciation in ninespine stickleback: reproductive isolation and phenotypic divergence among cryptic species of Japanese ninespine stickleback. *J Evol Biol.* **26**:1417–1430.
- Jones FC, Grabherr MG, Chan YF, Russell P, Mauceli E, Johnson J, Swofford R, Pirun M, Zody MC, White S, et al. 2012. The genomic basis of adaptive evolution in threespine sticklebacks. *Nature* **484**:55–61.
- Jones MR, Mills LS, Alves PC, Callahan CM, Alves JM, Lafferty DJR, Jiggins FM, Jensen JD, Melo-Ferreira J, Good JM. 2018. Adaptive introgression underlies polymorphic seasonal camouflage in snowshoe hares. *Science* **360**:1355–1358.
- Kalyaanamoorthy S, Minh BQ, Wong TKF, von Haeseler A, Jermiin LS. 2017. Modelfinder: fast model selection for accurate phylogenetic estimates. *Nat Methods.* **14**:587–589.
- Keivany Y, Nelson JS. 2000. Taxonomic review of the genus *Pungitius*, ninespine sticklebacks (Gasterosteidae). *Cybium* **24**:107–122.
- Keivany Y, Nelson JS. 2004. Phylogenetic relationships of sticklebacks (Gasterosteidae), with emphasis on ninespine sticklebacks (*Pungitius* spp.). *Behaviour* **141**:1485–1497.
- Kempainen P, Li Z, Rastas P, Loytynoja A, Fang BH, Yang J, Guo B, Shikano T, Merilä J. 2021. Genetic population structure constrains local adaptation in sticklebacks. *Mol Ecol.* **30**:1946–1961.
- Kingman GAR, Lee D, Jones FC, Desmet D, Bell MA, Kingsley DM. 2021. Longer or shorter spines: reciprocal trait evolution in stickleback via triallelic regulatory changes in *Stanniocalcin2a*. *Proc Natl Acad Sci U S A.* **118**:e2100694118.
- Lamichhaney S, Berglund J, Almen MS, Maqbool K, Grabherr M, Martinez-Barrío A, Promerova M, Rubin CJ, Wang C, Zamani N, et al. 2015. Evolution of Darwin's Finches and their beaks revealed by genome sequencing. *Nature* **518**:371–375.
- Li H, Durbin R. 2010. Fast and accurate long-read alignment with Burrows-Wheeler transform. *Bioinformatics* **26**:589–595.
- Li H, Durbin R. 2011. Inference of human population history from individual whole-genome sequences. *Nature* **475**:493–496.
- Li H. 2011. A statistical framework for SNP calling, mutation discovery, association mapping and population genetical parameter estimation from sequencing data. *Bioinformatics* **27**:2987–2993.
- Lin Q, Fan SH, Zhang YH, Xu M, Zhang HX, Yang YL, Lee AP, Woltering JM, Ravi V, Gunter HM, et al. 2016. The seahorse genome and the evolution of its specialized morphology. *Nature* **540**:395–399.
- Malinsky M, Matschiner M, Svardal H. 2021. Dsuite—fast D-statistics and related admixture evidence from VCF files. *Mol Ecol Resour.* **21**:584–595.
- Malinsky M, Svardal H, Tyers AM, Miska EA, Genner MJ, Turner GF, Durbin R. 2018. Whole-genome sequences of Malawi cichlids reveal multiple radiations interconnected by gene flow. *Nat Ecol Evol.* **2**:1940–1955.
- Martin SH, Jiggins CD. 2017. Interpreting the genomic landscape of introgression. *Curr Opin Genet Dev.* **47**:69–74.
- Medina P, Thornlow B, Nielsen R, Corbett-Detig R. 2018. Estimating the timing of multiple admixture pulses during local ancestry inference. *Genetics* **210**:1089–1107.
- Merilä J. 2013. Nine-spined stickleback (*Pungitius pungitius*): an emerging model for evolutionary biology research. *Ann N Y Acad Sci.* **1289**:18–35.
- Miller CT, Beleza S, Pollen AA, Schluter D, Kittles RA, Shriver MD, Kingsley DM. 2007. Cis-regulatory changes in kit ligand expression and parallel evolution of pigmentation in sticklebacks and humans. *Cell* **131**:1179–1189.
- Natri HM, Merilä J, Shikano T. 2019. The evolution of sex determination associated with a chromosomal inversion. *Nat Commun.* **10**:1–13.
- Nei M. 1987. *Molecular evolutionary genetics*. New York (NY): Columbia University Press.
- Nelson TC, Cresko WA. 2018. Ancient genomic variation underlies repeated ecological adaptation in young stickleback populations. *Evol Lett.* **2**:9–21.
- Nguyen LT, Schmidt HA, von Haeseler A, Minh BQ. 2015. IQ-TREE: a fast and effective stochastic algorithm for estimating maximum-likelihood phylogenies. *Mol Biol Evol.* **32**:268–274.
- Osipova E, Hecker N, Hiller M. 2019. Repeatfiller newly identifies megabases of aligning repetitive sequences and improves annotations of conserved non-exonic elements. *Gigascience* **8**:giz132.
- Pease JB, Haak DC, Hahn MW, Moyle LC. 2016. Phylogenomics reveals three sources of adaptive variation during a rapid radiation. *PLoS Biol.* **14**:e1002379.
- Pease JB, Hahn MW. 2015. Detection and polarization of introgression in a five-taxon phylogeny. *Syst Biol.* **64**:651–662.
- Peichel CL, Marques DA. 2017. The genetic and molecular architecture of phenotypic diversity in sticklebacks. *Philos Trans R Soc B Biol Sci.* **372**:20150486.
- Pfennig KS. 2021. Biased hybridization and its impact on adaptive introgression. *Trends Ecol Evol (Amst).* **36**:488–497.
- Quinlan AR, Hall IM. 2010. BEDTools: a flexible suite of utilities for comparing genomic features. *Bioinformatics* **26**:841–842.
- Raviner M, Yoshida K, Shigenobu S, Toyoda A, Fujiyama A, Kitano J. 2018. The genomic landscape at a late stage of stickleback speciation: high genomic divergence interspersed by small localized regions of introgression. *PLoS Genet.* **14**(5):e1007358.
- Rawlinson SE, Bell MA. 1982. A stickleback fish (*Pungitius*) from the Beogene Sterling Formation, Kenai Peninsula, Alaska. *J Paleontol.* **56**:583–588.
- Rosenblum EB, Parent CE, Brandt EE. 2014. The molecular basis of phenotypic convergence. *Annu Rev Ecol Syst.* **45**:203–226.
- Rosenthal G. 2013. Individual mating decisions and hybridization. *J Evol Biol.* **26**:252–255.
- Sankararaman S, Mallick S, Dannemann M, Prüfer K, Kelso J, Paabo S, Patterson N, Reich D. 2014. The genomic landscape of neanderthal ancestry in present-day humans. *Nature* **507**:354–357.
- Schluter D, Conte GL. 2009. Genetics and ecological speciation. *Proc Natl Acad Sci U S A.* **106**:9955–9962.
- Setter D, Mousset S, Cheng X, Nielsen R, DeGiorgio M, Hermisson J. 2020. Volcanofinder: genomic scans for adaptive introgression. *PLoS Genet.* **16**:e1008867.
- Shapiro MD, Bell MA, Kingsley DM. 2006. Parallel genetic origins of pelvic reduction in vertebrates. *Proc Natl Acad Sci U S A.* **103**:13753–13758.
- Shapiro MD, Summers BR, Balabhadra S, Aldenhoven JT, Miller AL, Cunningham CB, Bell MA, Kingsley DM. 2009. The genetic architecture of skeletal convergence and sex determination in ninespine sticklebacks. *Curr Biol.* **19**:1140–1145.
- Sharma V, Hiller M. 2017. Increased alignment sensitivity improves the usage of genome alignments for comparative gene annotation. *Nucleic Acids Res.* **45**:8369–8377.
- Shikano T, Laine VN, Herczeg G, Vilkki J, Merilä J. 2013. Genetic architecture of parallel pelvic reduction in ninespine sticklebacks. *G3: Genes Genomes Genetics.* **3**:1833–1842.
- Shikano T, Natri HM, Shimada Y, Merilä J. 2011. High degree of sex chromosome differentiation in stickleback fishes. *BMC Genomics.* **12**:474.
- Stern DL. 2013. The genetic causes of convergent evolution. *Nat Rev Genet.* **14**:751–764.
- Suarez HG, Langer BE, Ladde P, Hiller M. 2017. Chaincleaner improves genome alignment specificity and sensitivity. *Bioinformatics.* **33**:1596–1603.
- Suarez-Gonzalez A, Lexer C, Cronk QCB. 2018. Adaptive introgression: a plant perspective. *Biol Lett.* **14**:20170688.
- Suvorov A, Kim BY, Wang J, Armstrong EE, Peede D, D'Agostino ERR, Price DK, Waddell PJ, Lang M, Courtier-Orgogozo V, et al. 2022. Widespread introgression across a phylogeny of 155 *Drosophila* genomes. *Curr Biol.* **32**:111–123.e5.
- Takahashi H, Goto A. 2001. Evolution of east Asian ninespine sticklebacks as shown by mitochondrial DNA control region sequences. *Mol Phylogenet Evol.* **21**:135–155.
- Takahashi H, Moller PR, Shedko SV, Ramatulla T, Joen SR, Zhang CG, Sideleva VG, Takata K, Sakai H, Goto A, et al. 2016. Species

- phylogeny and diversification process of northeast Asian *Pungitius* revealed by AFLP and mtDNA markers. *Mol Phylogenet Evol.* **99**:44–52.
- Takahashi H, Takata K, Goto A. 2001. Phylogeography of lateral plate dimorphism in the freshwater type of ninespine sticklebacks, genus *Pungitius*. *Ichthyol Res.* **48**:143–154.
- Takahashi H, Takata K. 2000. Multiple lineages of the mitochondrial DNA introgression from *Pungitius pungitius* (L.) to *Pungitius ty-mensis* (Nikolsky). *Can J Fish Aquat Sci.* **57**:1814–1833.
- Takahashi H, Tsuruta T, Goto A. 2003. Population structure of two ecologically distinct forms of ninespine stickleback, *Pungitius pungitius*: gene flow regimes and genetic diversity based on mtDNA sequence variations. *Can J Fish Aquat Sci.* **60**:421–432.
- Taylor SA, Larson EL. 2019. Insights from genomes into the evolutionary importance and prevalence of hybridization in nature. *Nat Ecol Evol.* **3**:170–177.
- Than C, Ruths D, Nakhleh L. 2008. Phylonet: a software package for analyzing and reconstructing reticulate evolutionary relationships. *BMC Bioinformatics.* **9**:1–16.
- Tickle C, Cole NJ. 2004. Morphological diversity: taking the spine out of three-spine stickleback. *Curr Biol.* **14**:R422–R424.
- Tsuruta T, Goto A. 2006. Fine scale genetic population structure of the freshwater and Omono types of nine-spined stickleback *Pungitius pungitius* (L.) within the Omono River system, Japan. *J Fish Biol.* **69**:155–176.
- Vanderpool D, Minh BQ, Lanfear R, Hughes D, Murali S, Harris RA, Raveendran M, Muzny DM, Hibbins MS, Williamson RJ, et al. 2020. Primate phylogenomics uncovers multiple rapid radiations and ancient interspecific introgression. *PLoS Biol.* **18**:e3000954.
- Varadharajan S, Rastas P, Loytynoja A, Matschiner M, Calboli FCF, Guo B, Nederbragt AJ, Jakobsen KS, Merilä J. 2019. A high-quality assembly of the nine-spined stickleback (*Pungitius pungitius*) genome. *Genome Biol Evol.* **11**:3291–3308.
- Wang C, Shikano T, Persat H, Merilä J. 2015. Mitochondrial phylogeography and cryptic divergence in the stickleback genus *Pungitius*. *J Biogeogr.* **42**:2334–2348.
- Wang C, Shikano T, Persat H, Merilä J. 2017. Phylogeography and historical introgression in smoothtail nine-spined sticklebacks, *Pungitius laevis* (Gasterosteiformes: Gasterosteidae). *Biol J Linn Soc.* **121**:340–354.
- Wang Y, Wang Y, Zhao Y, Kravchenko AY, Merilä J, Guo B. 2022. Phylogenomics of northeast Asian *Pungitius* sticklebacks. *Divers Distrib.* **28**:2610–2621.
- Willis PM. 2013. Why do animals hybridize? *Acta Ethol.* **16**:127–134.
- Xie KT, Wang GL, Thompson AC, Wucherpfennig JJ, Reimchen TE, MacColl ADC, Schluter D, Bell MA, Vasquez KM, Kingsley DM. 2019. DNA fragility in the parallel evolution of pelvic reduction in stickleback fish. *Science* **363**:81–84.
- Yamasaki YY, Kakioka R, Takahashi H, Toyoda A, Nagano AJ, Machida Y, Moller PR, Kitano J. 2020. Genome-wide patterns of divergence and introgression after secondary contact between *Pungitius* sticklebacks. *Philos Trans R Soc B Biol Sci.* **375**:20190548.
- Yu Y, Dong JR, Liu KJ, Nakhleh L. 2014. Maximum likelihood inference of reticulate evolutionary histories. *Proc Natl Acad Sci U S A.* **111**:16448–16453.
- Zhang W, Dasmahapatra KK, Mallet J, Moreira GRP, Kronforst MR. 2016. Genome-wide introgression among distantly related *Heliconius* butterfly species. *Genome Biol.* **17**:1–15.